

## SUPPLEMENTARY MATERIALS

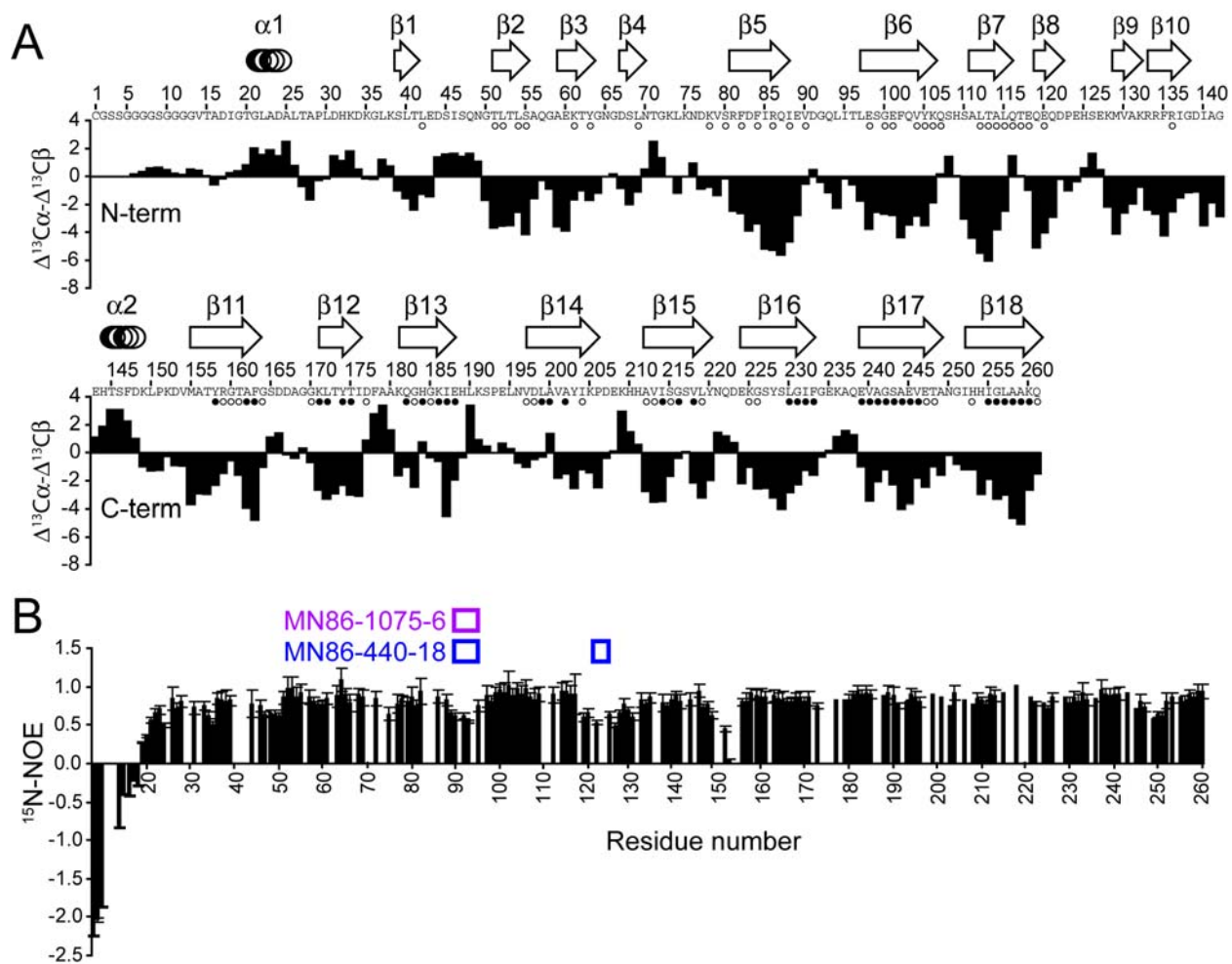
### **Structural basis for the immunogenic properties of the meningococcal vaccine candidate LP2086**

Alessandro Mascioni<sup>1</sup>, Breagh E. Bentley<sup>2</sup>, Rosie Camarda<sup>2</sup>, Deborah A. Dilts<sup>2</sup>, Pamela Fink<sup>2</sup>, Viktoria Gusarova<sup>2</sup>, Susan Hoiseth<sup>2</sup>, Jaison Jacob<sup>1</sup>, Shuo L. Lin<sup>2</sup>, Karl Malakian<sup>1</sup>, Lisa K. McNeil<sup>2</sup>, Terri Mininni<sup>2</sup>, Franklin Moy<sup>1</sup>, Ellen Murphy<sup>2</sup>, Elena Novikova<sup>2</sup>, Scott Sigethy<sup>2</sup>, Yingxia Wen<sup>1</sup>, Gary W. Zlotnick<sup>2</sup> and Désirée H. H. Tsao<sup>1</sup>

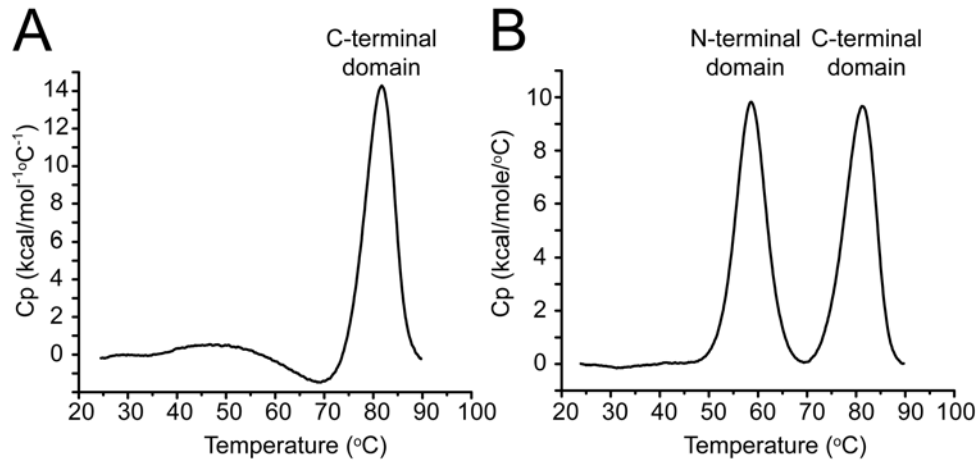
<sup>1</sup> Wyeth Research, Structural Biology and Computational Chemistry, 200 Cambridge Park Drive, Cambridge, MA, 02140

<sup>2</sup> Wyeth Vaccines Research, 401 North Middletown Road, Pearl River, NY 10965

Correspondence should be addressed to D. H. H. T. (dtsao@wyeth.com) or G. W. Z. (zlotnig@wyeth.com).

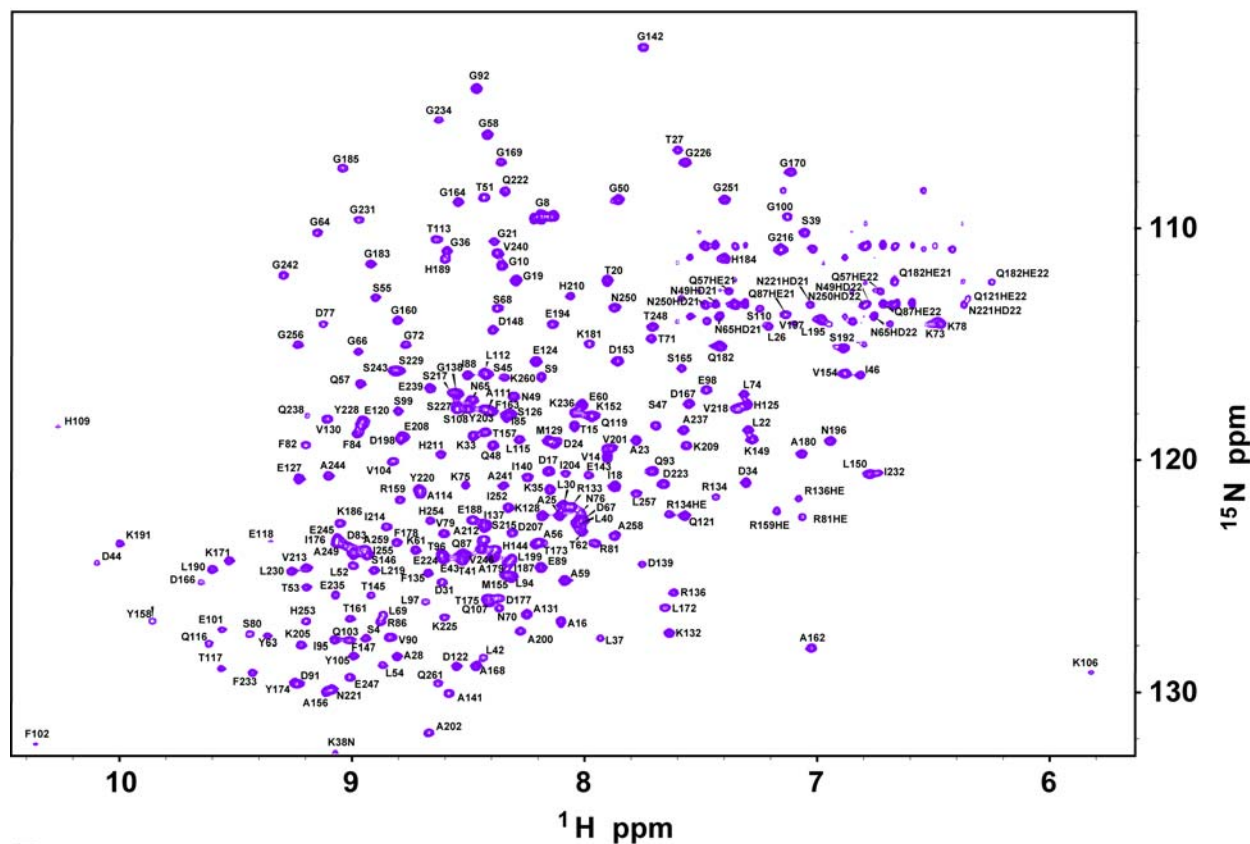


**Supplementary Figure 1** Secondary structure, D<sub>2</sub>O exchange and relaxation experiments for LP2086-B01. **(a)** Solid bars indicate deviations of the  $^{13}\text{C}\alpha$  and  $^{13}\text{C}\beta$  chemical shifts from the random coil values. Negative deviations are indicative of  $\beta$ -strands while positive deviations correspond to  $\alpha$ -helices. The circles mark hydrogen bond constraints used in the calculation. Open circles represent protons that exchanged with deuterium in 60% D<sub>2</sub>O buffer. Solid circles correspond to backbone deuterons that did not exchange back with protons following the expression of the protein in perdeuterated media. **(b)** Backbone mobility as indicated by heteronuclear  $^{15}\text{N}$ -NOE relaxation. mAb MN86-1075-6 and MN86-440-18 (magenta and blue respectively) target epitopes corresponding to flexible loops at the N-domain. Two ranges of fluctuation of the backbone dynamics are observed for the C- and the N-domains. Excluding the flexible loop 248–252, the average  $^{15}\text{N}$ -NOE for the  $\beta$ -barrel is  $0.87 \pm 0.08$ . The most dynamic residues in the inter-domain linker are Val154 and Asp153, with values of NOE relaxation of  $0.02 \pm 0.02$  and  $0.46 \pm 0.03$  respectively. The most rigid residue in the linker is Phe147 with NOE of  $0.94 \pm 0.09$ . The N-domain  $^{15}\text{N}$ -NOE relaxations fluctuate over a broader range, with an average value of  $0.89 \pm 0.11$  for the regions enclosing the hydrophobic core (51–58 in  $\beta 2$ , 61–72 in  $\beta 3$ , 78–88 in  $\beta 4$ , and 97–118 in  $\beta 5$  and  $\beta 6$ ). The remaining regions of the N-domain have heteronuclear NOE below 0.7. Overlapped peaks are excluded from graph. Data in **b** are means from three samples. Error bars indicate s.d.

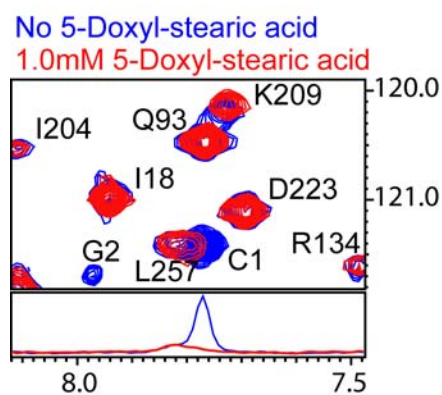


**Supplementary Figure 2** DSC experiments on the full length LP2086-B01 and the C-terminal  $\beta$ -barrel domain (residues 107–261). **(a)** For the C-terminal domain of LP2086-B01, one single thermal transition is observed at 82°C. **(b)** For the full length LP2086-B01 two transitions are observed at 59°C and 82°C corresponding to melting of the N- and C-domains, respectively.

A

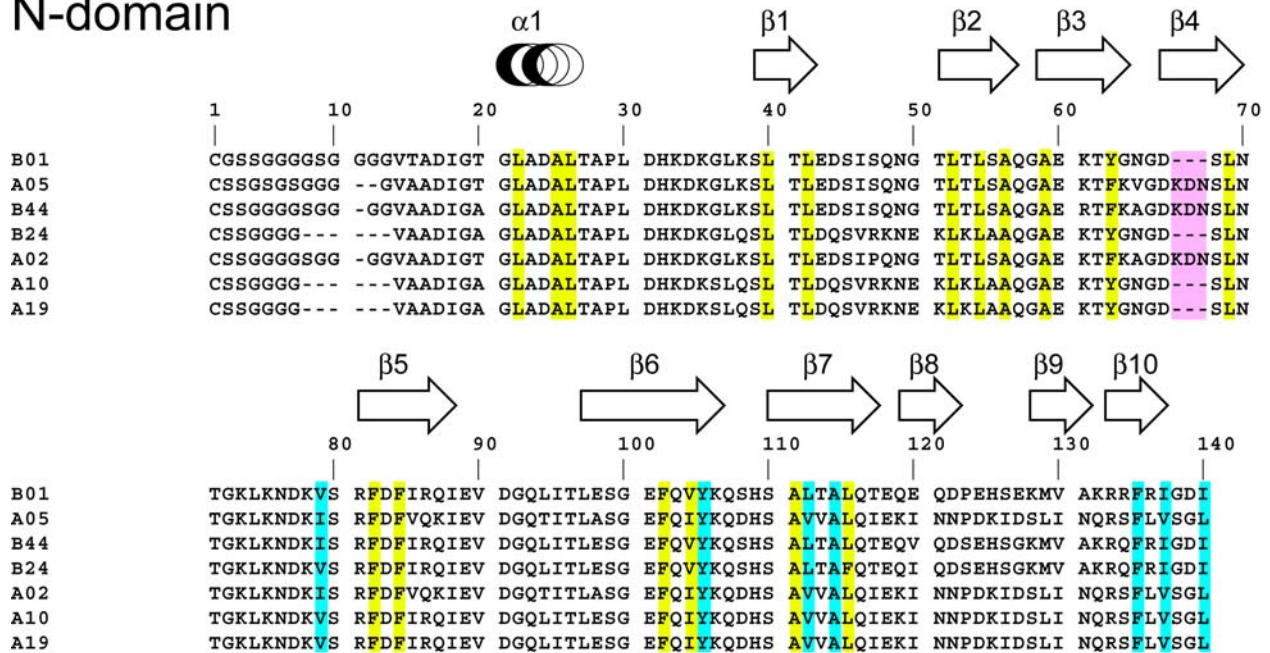


B

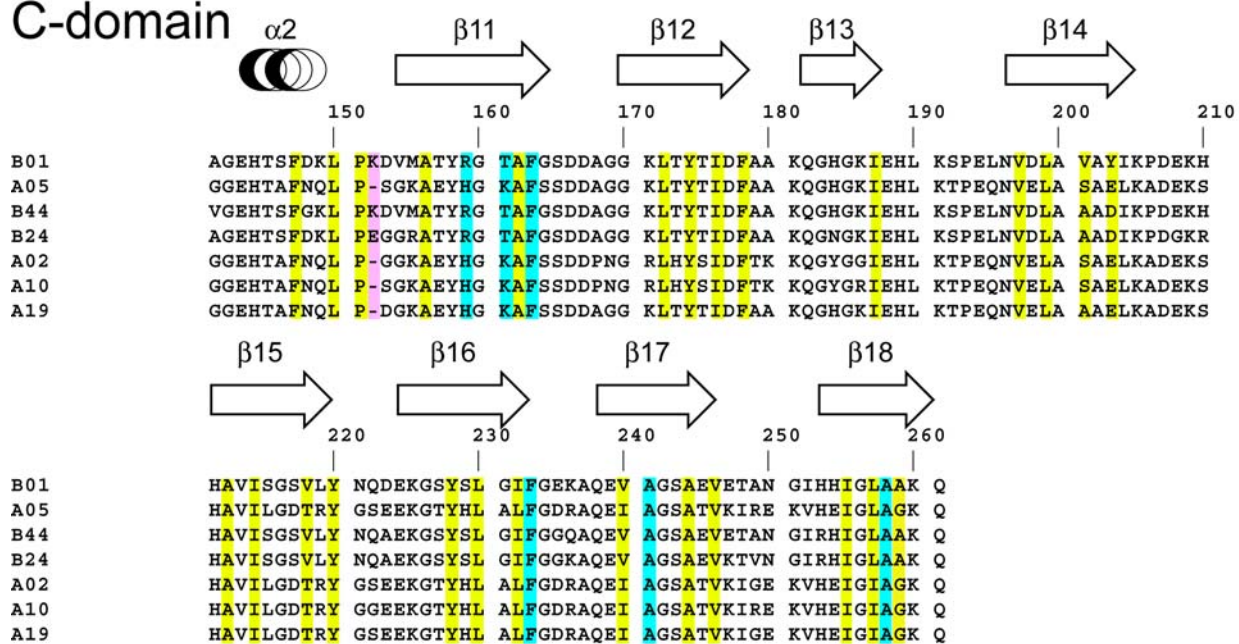


**Supplementary Figure 3** Assigned TROSY spectra of the lipidated LP2086-B01 in 30 mM Zwittergent 3–12 at pH 7.4. **(a)** Assigned TROSY spectra. In the lipidated sample in micellar solution, intermolecular NOEs between the N-terminal residues Cys1 and Gly2, and the detergent head-groups and the lipid tails of the palmitoyl fatty acids, are identified on the  $^{15}\text{N}$ -NOESY. **(b)** Paramagnetic quenching with 5-doxyl-stearic acid. Blue: no 5-doxyl-stearic acid, and Red: 1.0 mM 5-doxyl-stearic acid. Due to its property to reconstitute into the micelle with the 5-doxyl free radical positioned below the detergent head-groups, this reagent induces selective paramagnetic line broadening of residues bound to the micellar surface<sup>16,17</sup>. At 1.0 mM 5-doxyl-stearic acid, the resonances of the N-terminal residues Cys1 and Gly2 are quenched beyond detectability. The remaining peaks on the spectra are not affected by the presence of the paramagnetic reagent.

## N-domain



## C-domain



**Supplementary Figure 4** Sequence alignment of selected variants from subfamily A and B of LP2086. The sequence numbering is referenced to the Cys1 of LP2086-B01. A higher degree of sequence identity is observed over the N-terminal domain (1–140) versus the C-terminal domain (154–261). Residues colored in yellow form the hydrophobic cores of the two domains, and are highly conserved across the two subfamilies. Sequence identity is also observed for the two hydrophobic patches (light blue) with the exception of the two variations R159H and T161K.